

Supplementary information Section

A step ahead towards the green synthesis of monodisperse gold nanoparticles: the use of crude glycerol as a greener and low-cost reducing agent

Rashida Parveen^a and Germano Tremiliosi Filho^{a*}

^a Institute of Chemistry of São Carlos, University of São Paulo, P.O. Box 780, CEP 13560-970, São Carlos, SP, Brazil

*Corresponding Author: germano@iqsc.usp.br (G.T Filho); Phone: +55-163373-9951

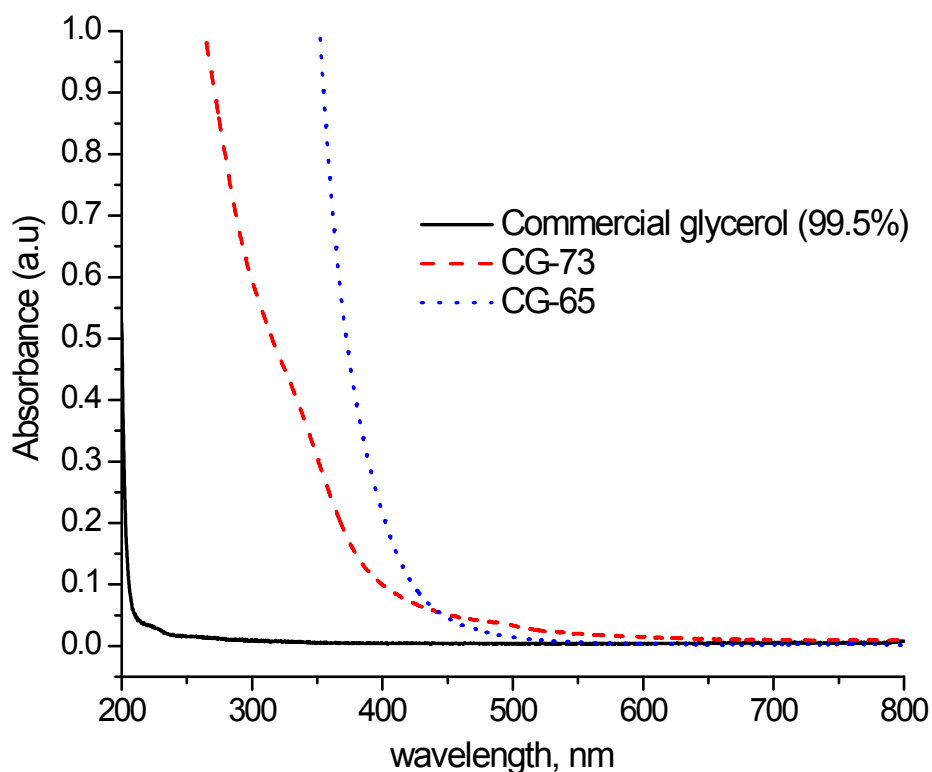


Fig. S1: UV-Visible spectrum of pure glycerol (black curve), CG-73 (red curve) CG-65 (blue curve).

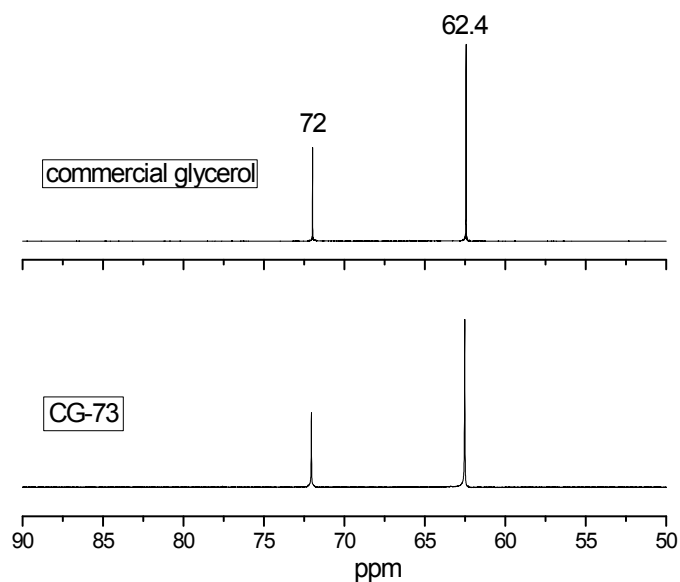


Fig. S2: ^{13}C -NMR spectrum of commercial glycerol (above) and CG-73 after simple filtration through a $0.2\ \mu\text{m}$ syringe-fitted filter (below).

The ^{13}C -NMR spectrum (Fig. S2) of commercial glycerol (Panreac) demonstrates two signals at 62.4 ppm and 72.0 ppm which are assigned to the primary and secondary aliphatic carbon atoms, respectively. The spectrum of CG-73 shows the same peaks at the same position as the pure commercial glycerol and no additional peaks are observed. This shows the absence of any significant quantity of organic impurities, in agreement with the FTIR analysis (Fig. S3)

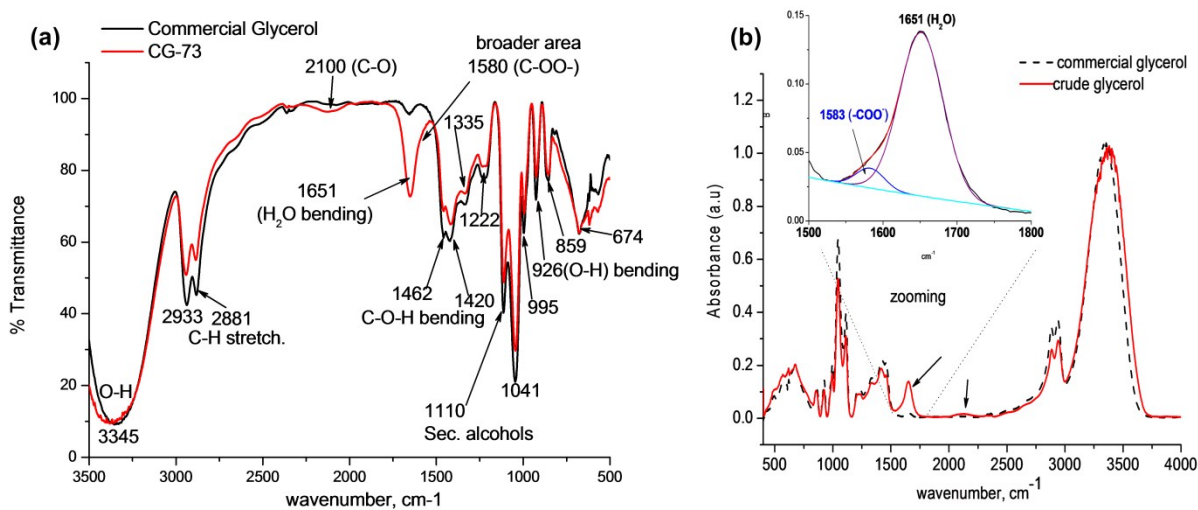


Fig. S3: (a) FTIR spectrum of CG-73 as compared to commercial glycerol (99.5 %) and (b) the same spectra in absorption mode zoomed in the region 1500–1800 cm^{-1} to show the details of the bands in this region (inset). Various vibrational modes have been marked in the Fig.

The FTIR spectra of both CG-73 and commercial glycerol are almost similar and shows peaks at 3345 cm^{-1} (O-H stretching), $2933\text{--}2881\text{ cm}^{-1}$ (C-H stretching), 1652 cm^{-1} (H_2O bending), $1420\text{--}1460\text{ cm}^{-1}$ (C-O-H bending), 1110 cm^{-1} (C-O stretching of secondary alcohols) and 926 cm^{-1} (O-H bending). The FTIR spectra of CG-73, however, shows a prominent and broader feature centered at 1651 cm^{-1} . This broad band between $1500\text{--}1800\text{ cm}^{-1}$ can be resolved into two components, the components at 1583 cm^{-1} being assigned to the -COO^- functionality (Fig. S3b). Thus traces of fatty acids or soap may be present in CG-73 sample.

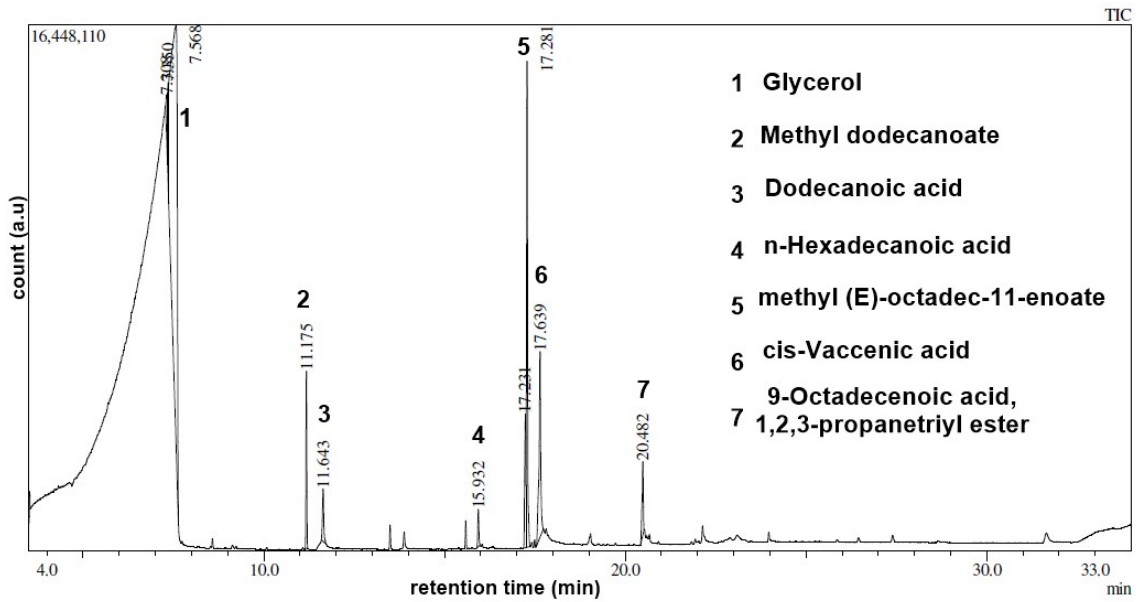


Fig. S4: Gas chromatogram of CG-65 sample. The compounds responsible for these peaks, as identified from mass spectrograms (Fig. S5) have been denoted on the RHS of the figure.

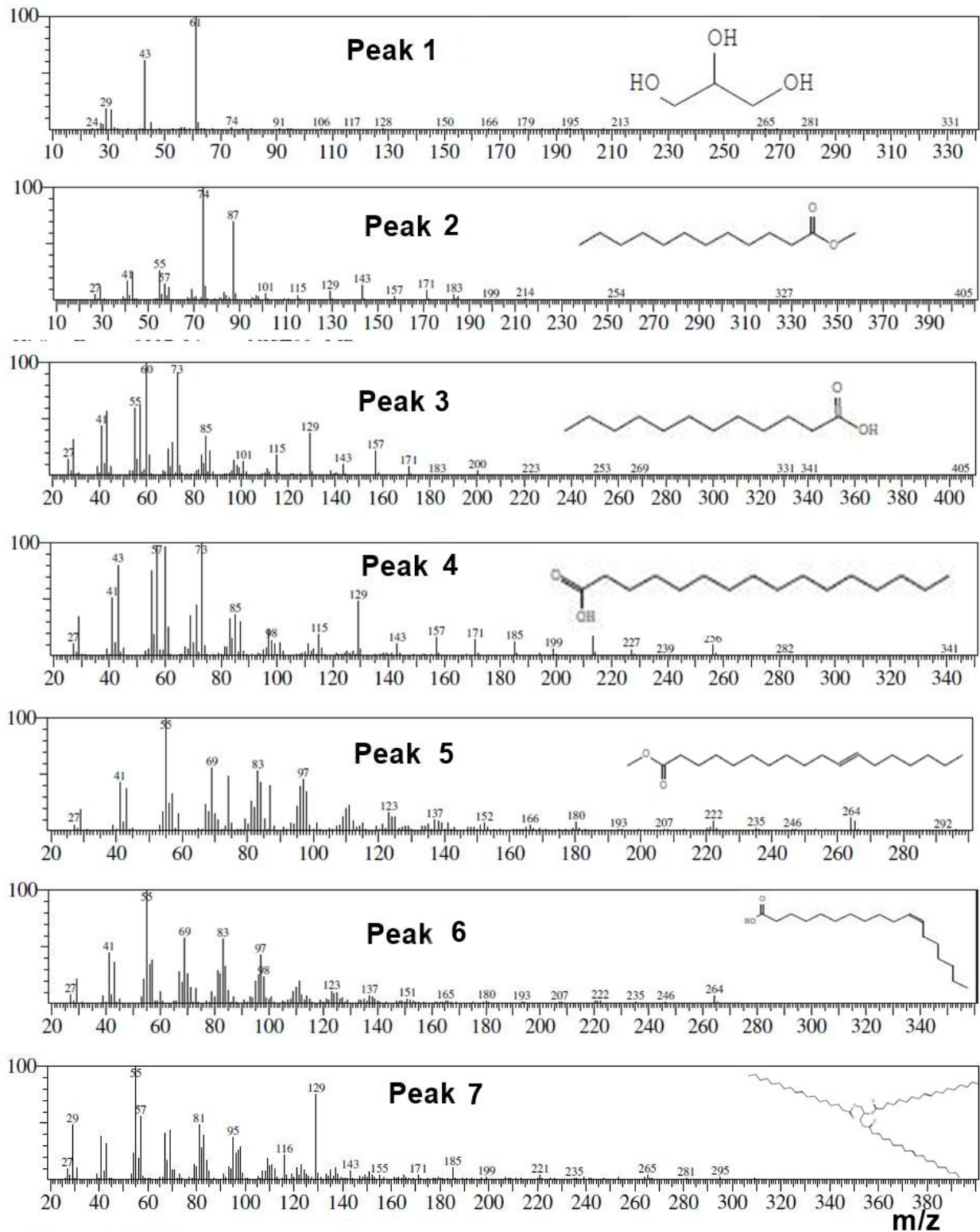


Fig. S5: Mass spectra of separated components in CG-65 sample. The chemical structures of corresponding compounds, as identified by MS, have also been shown.

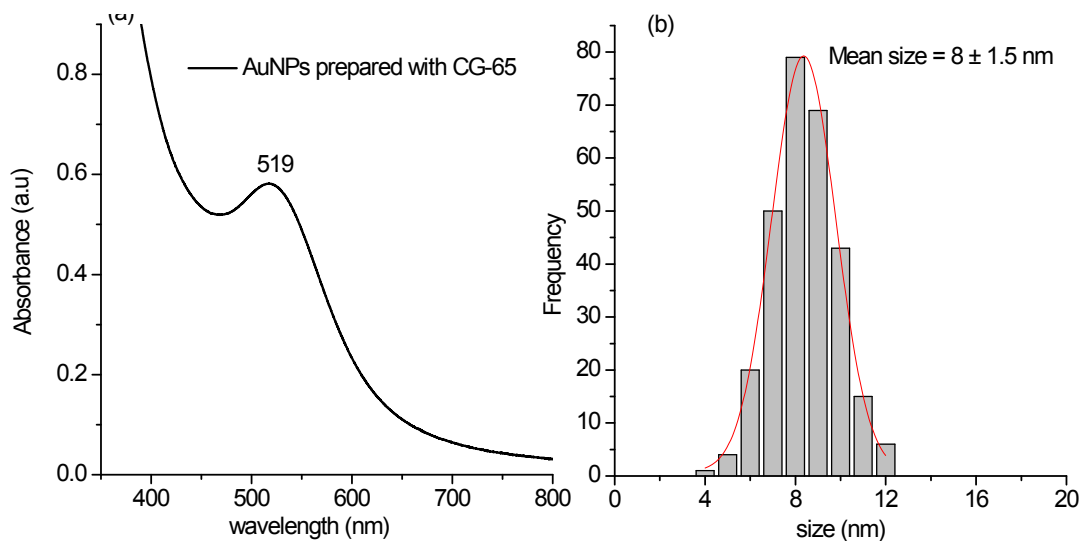


Fig. S6: (a) UV-Visible spectrum and (b) particle size distribution as measured by TEM of AuNPs prepared using CG-65. Conditions of synthesis 3.75×10^{-3} mmols HAuCl_4 , 1% PVP and 13.2 pH.

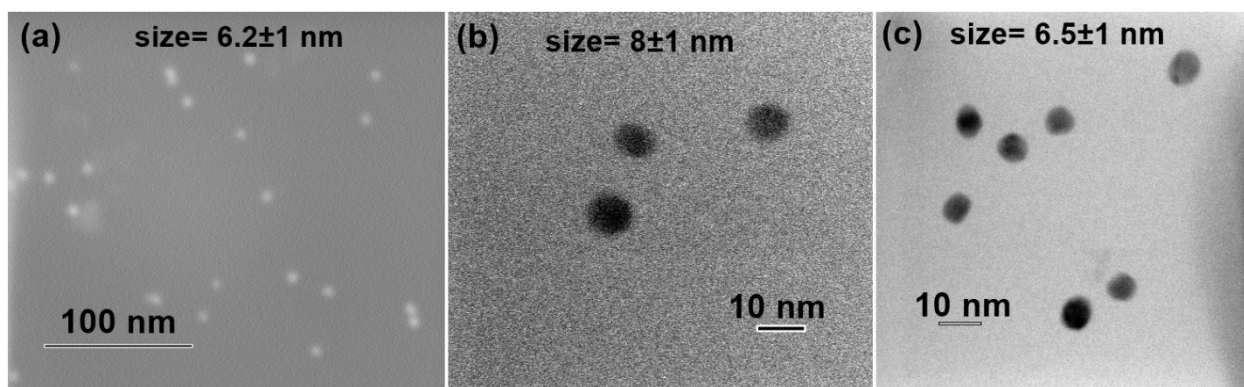


Fig. S7: (a) SEM image of AuNPs prepared using 0.1 mol L^{-1} CG-73 and TEM images of AuNPs prepared using (b) 0.2 mol L^{-1} and (c) 0.4 mol L^{-1} CG-73. The average particle size of AuNPs along with standard deviation has been indicated above each image.

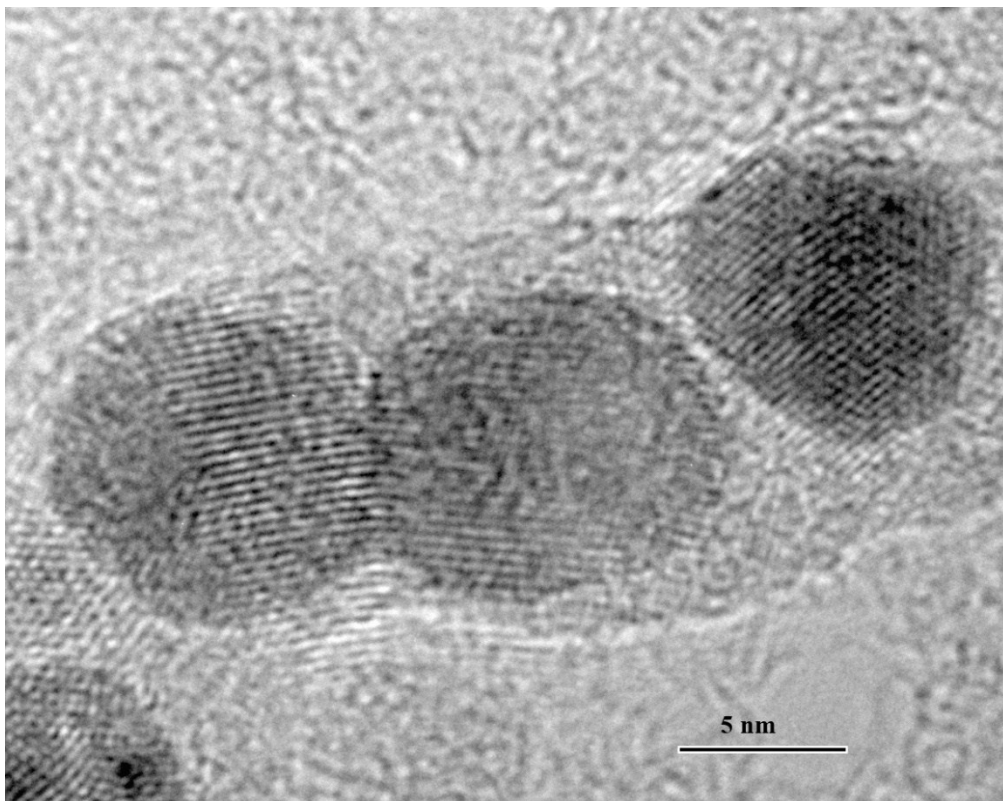


Fig. S8: Representative high resolution TEM image of AuNPs prepared using CG-73

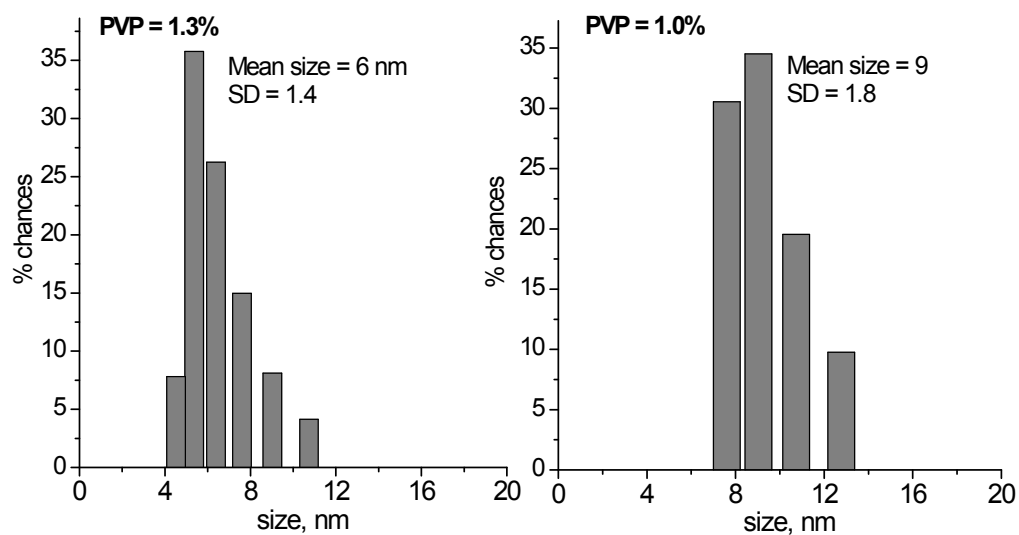


Fig. S9: DLS measurements of AuNPs prepared using different PVP concentration at fixed pH (~13.2), fixed glycerol (0.2 mol L⁻¹) and fixed H₂AuCl₄ (3.75 x 10⁻³) concentration. SD stands for standard deviation, which represents the breadth of size distribution of AuNPs

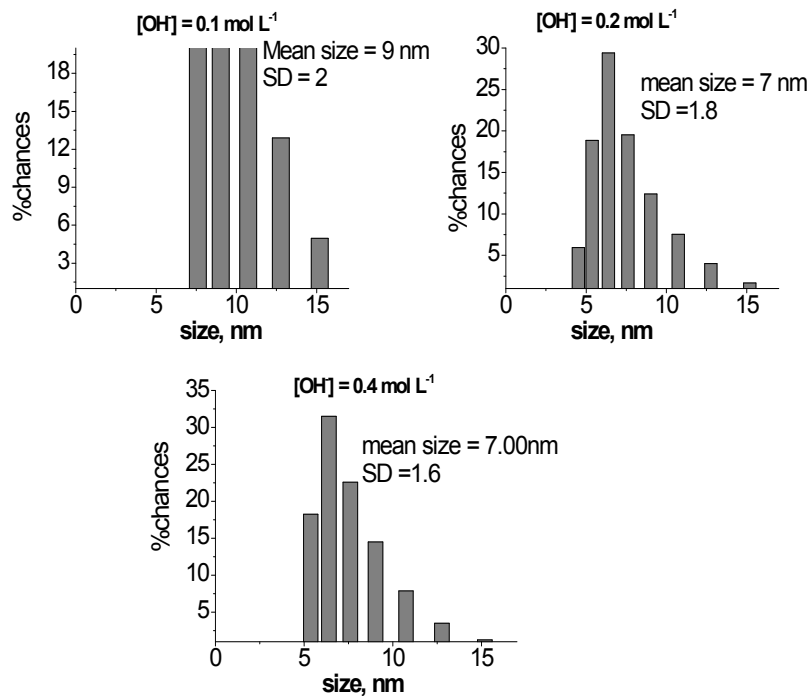


Fig. S10: Hydrodynamic diameter of AuNPs prepared using different OH^- concentrations at fixed PVP concentration (1 %), fixed glycerol (0.2 mol L^{-1}) and fixed HAuCl_4 ($3.75 \times 10^{-3} \text{ mmoles}$) concentration. SD stands for standard deviation, which represents the width of size distribution of AuNPs

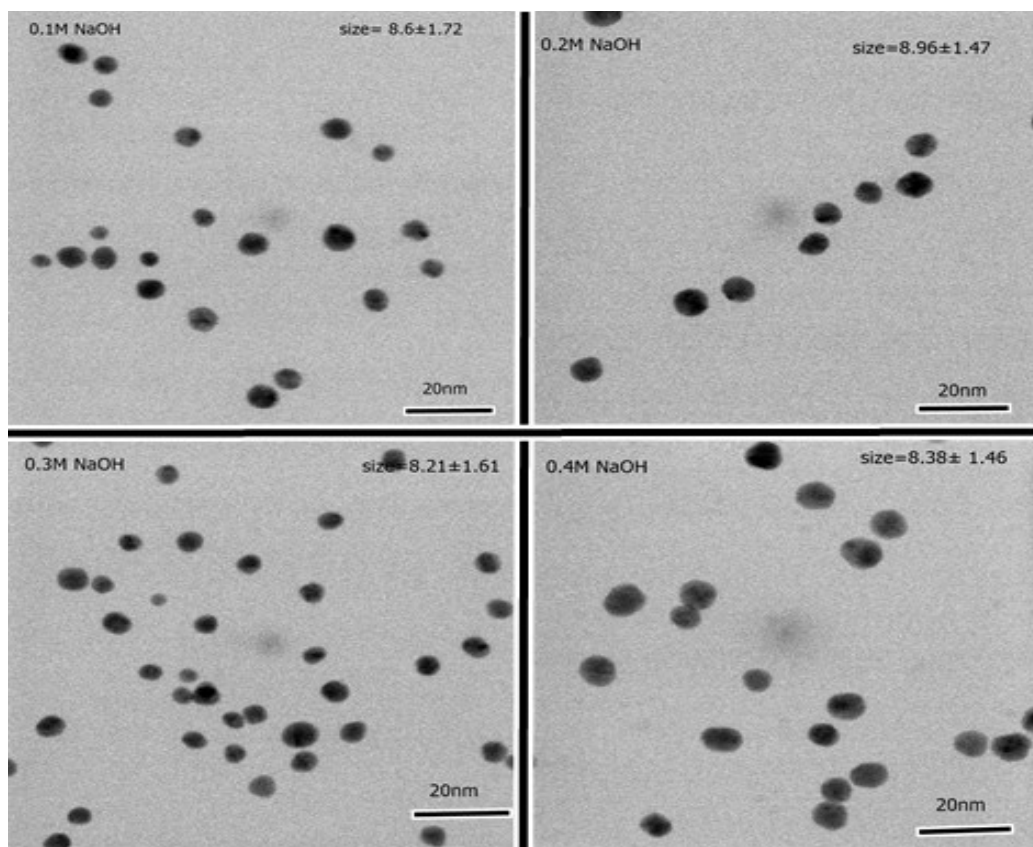


Fig. S11: TEM images of PDAC-stabilized AuNPs prepared using different pH while keeping other parameters constant. The letter M denotes concentration in mol L⁻¹.

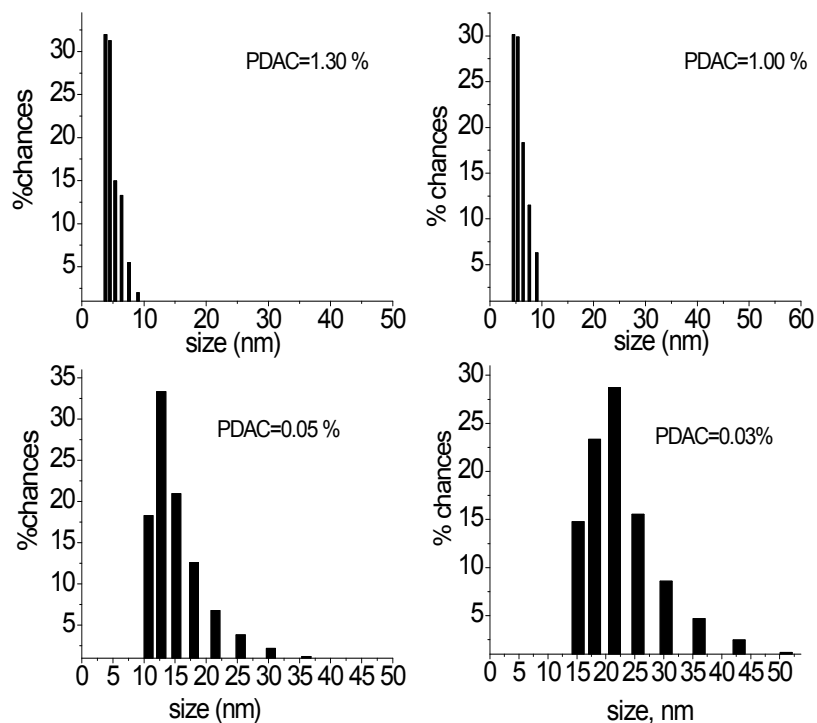


Fig. S12: DLS particles size distribution of PDAC-stabilized AuNPS obtained using different concentration of PDAC; all other experimental conditions are the same for each sample.

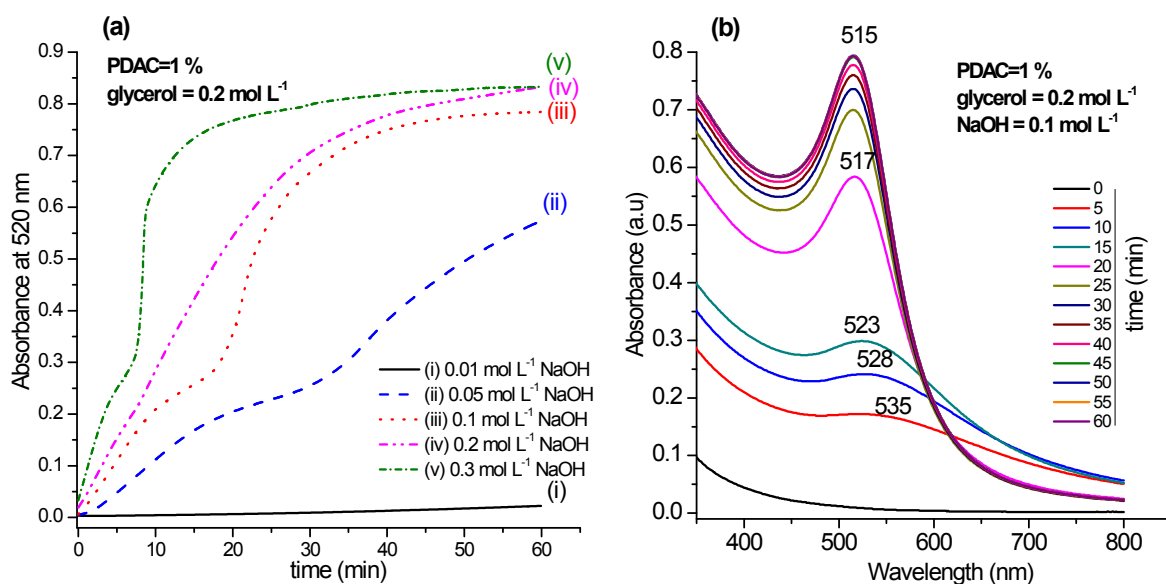


Fig. S13: (a) Time evolution of the absorbance band at 520 nm as function of pH in presence of both 1% PDAC and 0.2 mol L⁻¹ glycerol and (b) complete electronic absorption spectra taken at 0 min through 60 min at 05 minutes interval of PDAC-stabilized AuNPs (sample (iii) in Fig S13a) prepared using 0.1 mol L⁻¹ NaOH, 1% PDAC, 0.2 mol L⁻¹ glycerol and 3.75 x 10⁻³ mmole HAuCl₄.

Fig. S13a shows the temporal changes in the absorbance of the SPR band at 520 nm. It can be observed that growth of AuNPs is very slow at NaOH of 0.01 mol L⁻¹ or lower. The curves show a sharp increase in absorbance at higher NaOH concentration (NaOH > 0.01 mol L⁻¹). The slope of the absorbance curves shows a decrease at some point (at 18 min in curve (iii) and 6 min in curve (v), for example). Considering the fact that absorbance at only 520 nm is measured, this change in slope is related to the change in particle size and corresponding change in absorption wavelength as the reaction proceeds. Fig. S13b clearly shows the shift in optical spectra or absorption maximum for the sample prepared using 0.1 mol L⁻¹ NaOH.

Preparation of AgNPs using crude glycerol (CG)

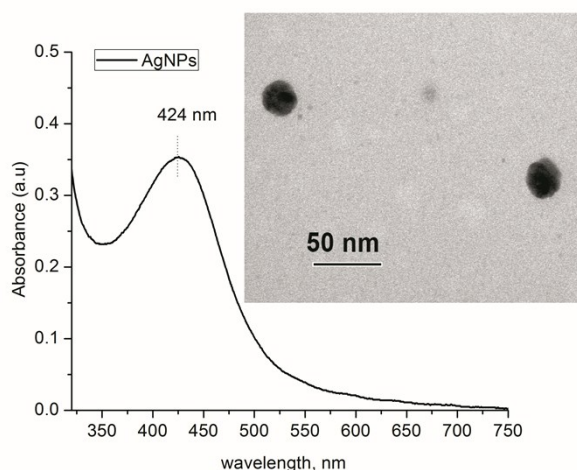


Fig. S14: UV-Visible spectrum and TEM images (inset) of AgNPs prepared using crude glycerol as reducing agent. Synthesis conditions: 20 μ L AgNO₃ (0.005 mol L⁻¹), 1 mL crude glycerol (0.2 mol L⁻¹ prepared in 0.8 mol L⁻¹ NaOH solution) and 1 mL PVP (1%).

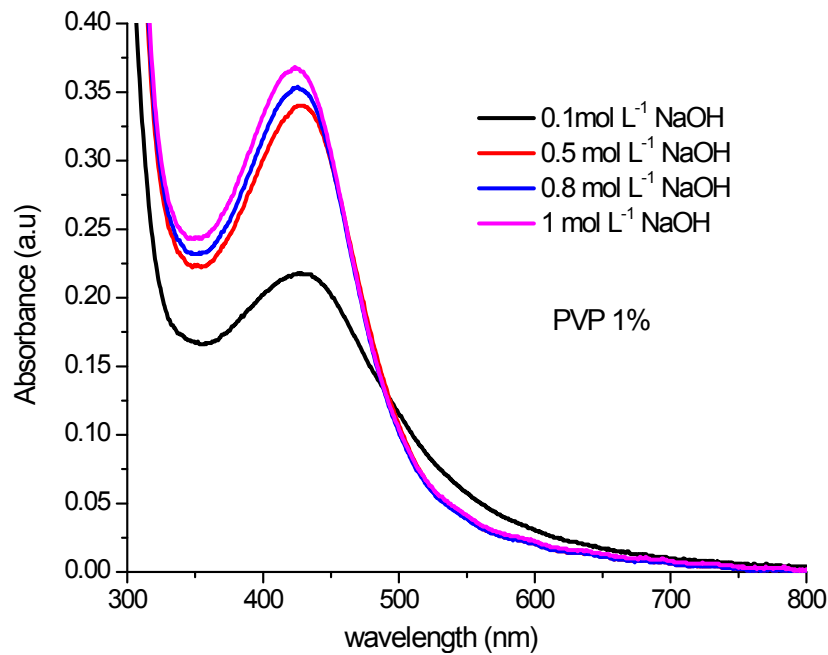


Fig. S15: UV-Visible spectra of AgNPs prepared using crude glycerol in the presence of different concentrations of NaOH under otherwise identical conditions. Synthesis conditions: 20 μL AgNO_3 (0.005 mol L^{-1}), 1 mL crude glycerol (0.2 mol L^{-1} prepared in NaOH solution of varying concentration) and 1 mL PVP (1%).